Alma Mater Studiorum Università di Bologna
Archivio istituzionale della ricerca

Single-material organic solar cells with fully conjugated electron-donor alkoxy-substituted bithiophene units and electron-acceptor benzothiadiazole moieties alternating in the main chain

Single-material organic solar cells with fully conjugated electron-donor alkoxy-substituted bithiophene units and electron-acceptor benzothiadiazole moieties alternating in the main chain

Martina Marinelli[a], Massimiliano Lanzi[a], Andrea Liscio[b], Alberto Zanelli[c], Mattia Zangoli[c], Francesca Di Maria[c,d*], Elisabetta Salatelli[a,*]

[a]   Dpt. of Industrial Chemistry Toso Montanari, University of Bologna, Viale del Risorgimento 4, I-40136 Bologna, Italy

[b]   CNR-IMM, Via del Fosso del Cavaliere 100, I-00133 Roma, Italy

[c]   CNR-ISOF, Via P. Gobetti 101, I-40129 Bologna, Italy

[d]   Mediteknologysrl, Via P. Gobetti 101, I-40129, Bologna, Italy

[*]   Corresponding authors: elisabetta.salatelli@unibo.it (E. Salatelli)

                           francesca.dimaria@isof.cnr.it (F. Di Maria)

ABSTRACT:Main chain conjugated linear polymers, constituted by alternating electron-donor (D) and -acceptor (A) moieties, have been prepared with the aim of testing their performances as photoactive components in single material organic solar cells (SMOSCs). The D moiety is constituted by bithiophene co-units bearing in the position 3of the thiophene ring an hexyloxy, a hexyloxymethyl or a hexyl group, while the A moiety is represented by the benzothiadiazole group. The D–A polymers were obtained in high yield through the poorly demanding oxidative $FeCl_3$ polymerization process - starting, respectively, from the related precursors 4,7-bis(3-hexyloxythiophen-2-yl)benzo[c][2,1,3]thiadiazole, 4,7-bis[3-(6-methoxyhexyl)thiophen-2-yl]benzo[c][2,1,3]thiadiazole and 4,7-bis(3-hexylthiophen-2-yl)benzo[c][2,1,3]thiadiazole - with low dispersity indexes, close to the monodisperse state, after fractionation with methanol. The materials have been thoroughly characterized for their physical and structural properties and then tested for photoconversion efficiency in SMOSCs by using different deposition procedures of the photoactive component. In agreement with Kelvin probe force microscopy (KPFM) measurements, the best photovoltaic performance was observed for the polymer based on conjugated 3-alkoxythiophene and benzothiadiazole moieties, achieving significant photocurrents for this type of fully conjugated alternating D–A structures ($Jsc = 2.63\text{-}3.72$ mA cm^{-2}).

1.   INTRODUCTION

Polymeric solar cells (PSCs) have been widely investigated in the past decades for their attractive combination of unique properties such as flexibility, lightweight, low cost and production easiness.[1] PSCs are generally constituted by a bicontinuous interpenetrating network -made of a conjugated polymer acting as electron donor (D) and an electron acceptor moiety (A) -capable of absorbing sunlight, producing excitons and generating electrical charges that can migrate to the electrodes.[1-3] A blended structure, namely bulk hetero-junction (BHJ), is currently adopted as the standard architecture for organic PSCs. Regioregular poly(3-alkylthiophene)s (P3AT)s thanks to their high solubility, film-forming ability and structural versatility have been the most studied and promising D materials in BHJ PSCs, with [6,6]-phenyl C61 methyl butyrate(PCBM) as the A counterpart.[3,4] However, their relatively large band gap limits the amount of solar light that can be absorbed. Therefore, researchers are actively synthesizing polymers with a narrower band gap, higher carrier mobility and a wider absorption up to the near infrared region.[5-10] It has been proved that the synthesis of conjugated copolymers combining D and A units within the same macromolecule is a powerful strategy to obtain low band gap materials, since the intramolecular charge transfer mechanism in D–A structure allows the extension of the conjugation length and affects the band gap values leading to the formation of new high-lying HOMO and low-lying LUMO energy levels.[5-10]Recently, D–A polymers were also employed as photoactive materials for the construction of single-material organic solar cells (SMOSCs), i.e. cells in which the photon-to-electron conversion process is ensured by one material in which D and A units are covalently linked.[11,12] The development of solar cells that employ a single material is highly promising since it could significantly reduce the complexity and cost of cell fabrication while overcoming the issue related to the morphological instability of

multicomponent BHJs.[13-15] For this purpose, several materials have been designed in the last years that differ essentially for the nature of D and A moieties, and, in particular, in their connection mode which determines the different intra- and intermolecular interactions.[12,16-21] TheD and A moieties can be covalently linked by a flexible insulating spacer, such as in "double- cable" systems, or by different conjugated bridges such as acetylenic, aromatic, olefinic (D–π– A) or directly (D–A), as in "in chain" D–A systems.[16-21] We have recently reported that "in chain" D–A oligomers and polymers, alternating "sulfur-overrich" bis(3,′4 -S-alkyl)-2,2′- bithiophenes as D units and 2,1,3-benzothiadiazoles, as A units, display photovoltaic behavior in

SMOSCs devices with power conversion efficiencies in the 0.24 .54% range.[22] Up to now,

these materials are among the few examples of fully conjugated D–A structures that lead to SMOSCs with significant photocurrents (Jsc = 1.70-2.40 mA cm^{-2}), a most interesting result since in these systems it was expected to be difficult to achieve an efficient nanophase separationbetween D and A moieties, with a consequent fast charge recombination and consequential low photocurrents.[12] It is important to note that only two other examples with a similar architecture are reported to work in SMOSCs, i.e., a triphenylamine-oligothiophene conjugated system and a DPP-thieno-TTF copolymer.[23,24] At present, polymers with a D–A–D–A sequence display lower efficiencies compared to block copolymers (DDDD–AAAA) and double cable polymers (A~DDDD~A).[16-21]However, only in fully conjugated molecular D–A systems it is possible to investigate the structural factors and minimal size of a D–A system capable of dissociating excitons. We report here a novel family of fully conjugated "in chain" D–A polymeric systems working as single materials in SMOSCs capable of reaching efficiencies up to ~ 0.8% with Jsc of 3.72 mA cm^{-2}. We synthesized a polymer based on conjugated 3-alkoxythiophene and benzothiadiazole moieties, as D and A building blocks respectively (P3a), and other two

4

polymers that differ in the substitution of the side chain of the D group: in one case is present an oxygen atom in a non-conjugated position relative to the thiophene unit (P3b), thus neutralizing its electronic effect, while in the other it is absent (P3c) (Scheme 1). The structural, electrochemical and photophysical properties of the polymers were investigated by differential scanning calorimetry (DSC), thermogravimetric analysis (TGA), ^{1}H-NMR, ultraviolet-visible (UV-Vis) and photoluminescence (PL) spectroscopy, as well as X-Ray diffractometry, cyclic voltammetry (CV), external quantum efficiency (EQE), atomic force microscopy (AFM) and Kelvin probe atomic force microscopy (KPFM). All polymers were finally tested as active media in air-processed SMOSCs. Due to charge recombination negatively affecting the device performance, a proper nanophase separation between D and A in SMOSCs is fundamental to simultaneously achieve an efficient exciton diffusion, charge separation and transport.[11,12] As this may be conditioned by the deposition process of the photoactive component, the spray coating method was also adopted for the preparation of the devices, as it shows great potential for large scale production,[25] and the results compared to those obtained by the usual doctor-blade deposition procedure. In particular, scanning probe measurements provide direct visualization of the formation of photogenerated charges and clearly show that the presence of clusters in spray- coated thin film plays a crucial role in increasing the performance of the device, underlining the importance of the grain boundaries and "disorder".

2. EXPERIMENTAL

Materials and methods. The synthetic procedure of the intermediates, monomers and polymers are available in the Supporting Information. 3-bromothiophene, 3-hexylthiophene, 2,1,3-benzothiadiazole-4,7-bis(boronic acid pinacol ester), sodium bicarbonate, sodium sulphate, potassium hydroxide, palladium(II)chloride dichloromethane complex (PdCl$_2$dppf), palladium-

5

tetrakis(triphenylphosphine) [Pd(PPh$_3$)$_4$], 3-methoxythiophene, 1-hexanol, *p*-toluenesulfonic acid monohydrate, *p*-methoxyphenol, 1,6-dibromohexane, [1,3-bis(diphenylphosphino)propane]dichloronickel(II) [Ni(dppp)Cl$_2$] were purchased from Sigma-Aldrich Co; *N*-bromosuccinimide and FeCl$_3$ were purchased from Fluka. All reagents and solvents were used as received. Organic solvents were dried by standard procedures.

TLC was carried out with 0.2-mm thick of silica gel 60 F$_{254}$ (Sigma). Preparative column chromatographies were carried out on glass columns with silica gel 60 (particle sizes 0.040-0.063 μm, Sigma).

Instruments. Microwave (MW) irradiation was performed in a MilestoneMicrosynthLabstation operating at 2450 MHz and equipped with pressure and temperaturesensors.

^{1}H-NMR and ^{13}C-NMR spectra were recorded on a Varian Mercury (400-500 MHz) spectrometer at room temperature in CDCl$_3$ solutions with TMS as the internal standard. Chemical shifts are given in ppm.

Molecular mass and dispersity of the polymers were determined in CHCl$_3$ by gel permeation chromatography (GPC) on a HPLC Lab Flow 2000 apparatus equipped with a Rheodyne 7725i injector, a PhenomenexPhenogel MXL type column and an RI K-2301 KNAUER detector. The calibration curve was obtained using monodisperse polystyrene standards.

Thermogravimetric analysis (TGA) of the polymers was carried out by a TGA TA Instruments Q600 apparatus operating under nitrogen atmosphere in the 20÷800°C temperature range at a heating scan rate of 20°C/min. A DSC TA Instruments Q2000 operating in the −50÷200°C temperature range at a heating rate of 10°C/min under nitrogen atmosphere was used for the thermal analyses by differential scanning calorimetry (DSC).

UV-Vis and photoluminescence spectra were run by using a Perkin Elmer Lambda 20 and Perkin Elmer LS50B spectrophotometer, respectively, at room temperature on 1.3 10^{-3} M chloroform solutions in 0.1 and 1 cm quartz cells. Solid state measurements were made on polymer samples cast from chlorobenzene solutions on quartz slides (5 mg mL^{-1}) by the doctor-blade technique or spray coating.

X-Ray diffraction analysis (XRD) was performed using a PANalyticalX'Pert diffractometer equipped with a copper anode (λmean = 0.15418 nm) and a fast X'Celerator detector on polymer samples deposited from chlorobenzene solutions on ITO (5 mg mL^{-1}) by the doctor-bladetechnique or spray coating.

Cyclic voltammetry measurements (CV) were performed at 0.1 V/s on an AMEL model 5000potentiostat/galvanostat controlled by the software Corrwere 2.9 for Windows. A home- made three- compartments electrochemical cell equipped with a Pt wire auxiliary electrode and an aq. KCl Saturated Calomel reference Electrode (SCE), both connected to the working compartment with a liquid bridge, was purged with Ar and maintained under Ar pressure during the measurements. The supporting electrolyte was 0.1 M $(C_2H_5)_4NBF_4$ (Sigma-Aldrich, puriss. vacuum dried) in anh. propylene carbonate (Sigma-Aldrich, stored under Ar pressure) where the oxidation potential of ferrocene resulted 0.50 V vs. SCE. Polymeric thin films were made by doctor-blade technique or spray coating from chlorobenzene solutions (5 mg mL^{-1}) on indium tin oxide (ITO) electrodes (2.25 cm^2) at room temperature. HOMO, LUMO and band gap (E_g) energies, expressed in eV units, were estimated on the basis of the following relationships: $E_{HOMO} = - (E_{ox} + 4.68)$, $E_{LUMO} = - (E_{red} + 4.68)$, $E_g = - (E_{HOMO} - E_{LUMO})$ where -4.68 eV is potential of SCE vs. the electron in the vacuum[26-28] that, taking into account the potential of the

liquid junction, corresponds to a ferrocene potential of about -5.1 eV in agreement with Cardona et al.[29-32]

Atomic force microscopy (AFM) and Kelvin probe force microscopy (KPFM) measurementswere performed in air by employing a commercial digital microscope Bruker MultiMode 8. In order to obtain a sufficiently large and detectable mechanical deflection, we used (k = 2.8 N/m) Pt/Ir coated Si ultra-levers (SCM-PIT, Bruker) with oscillating frequencies inthe range between 60-90 kHz. AFM and KPFM images were acquired in the same measurement; a topographic line scan is first obtained by AFM operating in semicontact mode and then that same line is rescanned in lift mode with the tip raised to a lift height of 20 nm. Images were acquired with typical scan-rate 10 $\mu m \cdot s^{-1}$. Raw AFM data were filtered to remove experimental artifacts by using histogram flattening procedures.[33] The KPFM technique provides a voltage resolution of about 5 mV and a lateral resolution of a few tens of nanometres.

External quantum efficiency (EQE) was measured by a 7-SC Spec III Modularized Solar Cell Spectral Test System (SevenStar Optics, Beijing, PRC). The J_{sc} values were calculated from the EQE curves according to Open Photovoltaics Analysis Platform. The thickness of the active layer was determined using a Burleigh Vista 100 AFM in a non-contact tapping mode. The reported photoconversion efficiency results were averaged from three different devices prepared under the same operating conditions with good reproducibility, with a standard deviation of about 5%.

Polymeric solar cells (PSC).PSC were fabricated on commercial ITO-coated glass substrates (2.5×2.5 cm, surface resistance 20 Ω/sq) according to the following procedure: the ITO layer was partially etched with acid (aq. HCl 10% wt.) and heated at 60°C for 15 min in order to obtain a final area of 1.5x1.0 cm covered by ITO. The substrate was then cleaned using distilled

water followed by 2-propanol, and finally dried by a gentle nitrogen flow. A conductive thin layer of poly(3,4-ethylenedioxythiophene):polystyrene sulfonic acid (Sigma-Aldrich, PEDOT:PSS, 2.8% wt., dispersion in water), diluted 1:1 v/v with isopropanol, was deposited using the doctor blade technique over the previously treated ITO glass and subsequently heated in a Büchi GKR-50 glass oven at 120°C for 2h under vacuum. The active layer constituted by the synthesized polymer sample was cast from chlorobenzene solution (5 mg mL^{-1}) by doctor-blade technique or spray coating and then annealead under vacuum at 120°C for 30 min. The device fabrication was completed by thermal evaporation of the Al electrode over the active layer through a shadow mask using an Edwards 6306A coating system operating at 10^{-6} mmHg (final active area of 1.0×1.0 cm). The current-voltage (I-V) characteristics and PCE were measured in air at room temperature using a Keithley 2401 source meter under the illumination of an Abet Technologies LS150 Xenon Arc Lamp Source AM 1.5 Solar Simulator (100 mW cm^{-2}), calibrated with an ILT 1400-BL photometer. The final structure of the device was: ITO (80 nm)/PEDOT:PSS (120 nm)/active layer (ca. 100 nm)/Al (50 nm).

3. RESULTS AND DISCUSSION

3.1 Synthesis and characterization of polymers P3a-c. The monomers 3a-c, employed for the synthesis of polymeric derivatives P3a-c, were obtained starting from 3-hexyloxythiophene (1a),[10] 3-(6-methoxyhexyl)thiophene (1b)[34] and 3-hexylthiophene (1c) (Scheme 1). In detail, precursors 1a-c were firstly treated with N-bromosuccinimide[35] to give the corresponding 2-bromo derivatives (2a-c) and then reacted with 2,1,3-benzothiadiazole-4,7-bis(boronic acid pinacol ester) via Pdcatalyzed Suzuki cross coupling. While monomers 3b-c were obtained with good yields from 2b-cby Pd(PPh$_3$)$_4$ catalyzed Suzuki coupling reaction, and thus through a different synthetic route with respect to that one reported in literature[36]for 3c, the synthesis of 3a

from 2a was carried out following the synthetic protocol based on microwave (MW) assistance,[37] recently adopted for similar benzothiadiazole derivatives,[22] with Pd(dppf)Cl$_2$ as catalyst. The implementationof MW irradiation allowed to obtain 3a in similar yields as 3b-c, but with a remarkable improvement of rate (30 min compared to 24 h), accompanied by a significant reduction of the reaction temperature (80°C vs. 110°C), with a consequent lower production of by-products.

Scheme 1. Synthetic route for the preparation of polymers P3a-c.
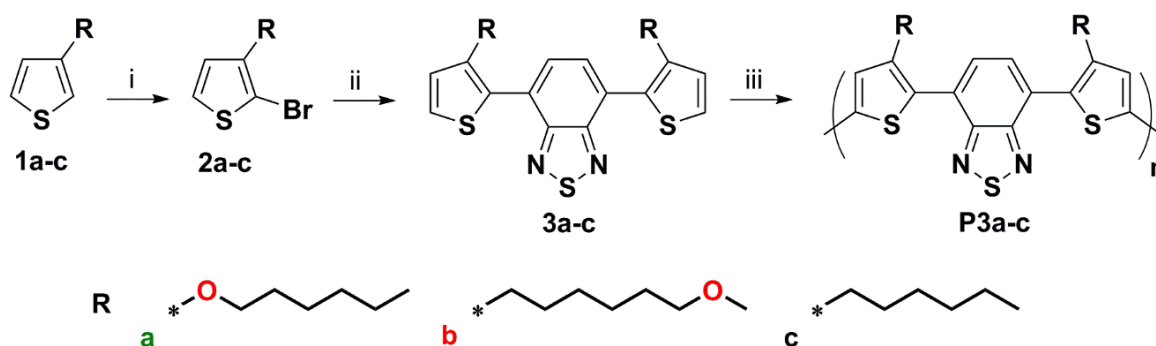
(i) 1 equiv of NBS, DMF, 0°C; (ii) 0.5 equiv of 2,1,3-benzothiadiazole-4,7-bis(boronic acid pinacolester), Pd(dppf)Cl$_2$, NaHCO$_3$, THF/H$_2$O 2/1, MW, 80°C for 3a; 0.5 equiv of 2,1,3-benzothiadiazole-4,7-bis(boronic acid pinacolester), Pd(PPh$_3$)$_4$, 2M K$_2$CO$_3$, toluene, reflux for 3b-c; (iii) 4 equiv of FeCl$_3$, CHCl$_3$.

The chemical structure of compounds 3a-c was confirmed by ^{1}H-NMR (Figure S1), which showed a significant downfield shift of the resonances of the aryl protons for 3a, if compared to the corresponding protons of 3b and 3c, indicative of an increased electron delocalization in the benzothiadiazole moiety due to the mesomeric effect of the oxygen atom directly linked to thiophene ring. The polymerization of 3a-c to obtain P3a-c derivatives was performed in good yields through a well established and straightforward oxidative coupling using FeCl$_3$. This procedure is a non-regiospecific method when applied to 3-alkylthiophenes, as it leads to polymers containing about 75% only of head-to-tail (HT) linkages; however, in the presented

cases it allows to obtain exclusively tail-to-tail (TT) junctions between the thiophene rings, as a consequence of the symmetrical structure and chemical equivalence of the coupling positions in the precursors. It is also worth noting that all samples, after purification, show values of the dispersity index close to the mono-disperse state, this uniformity in chain length may induce a favorable packing and nanoscale morphology for the separation of hole and electron transport. The ^{1}H-NMR spectra (Figure S10) confirm the expected structure of the polymeric samples, withP3a showing resonances for the aryl protons moved downfield with respect to those of the other samples, as already observed for the precursors 3a-c.

Table 1. Yields and characterization data of polymeric derivatives.

Polymer	Yield (%)[a]	M_n (g/mol)[b]	M_w/M_n[c]	x_n[d]	T_g (°C)[e]	T_d (°C)[f]
P3a	98	8600	1.1	17.3	43	238
P3b	79	15700	1.1	29.8	3	144
P3c	54	11800	1.2	25.3	1	139

[a] Weight of polymer/weight monomer x 100; [b] Average molecular weight determined by GPC in CHCl$_3$; [c] Dispersity index; [d] Average polymerization degree; [e] Glass transition temperature determined by DSC (second heating cycle); [f] Decomposition temperature determined by TGA.

As far as the thermal properties are concerned, P3a exhibits higher values of T_g and T_d than P3b and P3c despite its lower molecular weight, probably due to a more compact arrangement of the macromolecules in the solid state (Table 1). Moreover, the behavior of P3b results quite similar to that of P3c, evidencing that the presence of methoxy groups in the side chains does not substantially affect the T_g and T_d values in the bulk (Figures S11 and S12). In all cases, the presence of only glass transitions suggests that all the examined polymeric samples are predominantly in the amorphous state. Accordingly, X-Ray diffraction measurements carried out on P3a-c powders confirm the absence of any crystallinity in the bulk (Figure S14).

3.2 Optical and electrochemical characterization. As commonly observed in alternating D–A polymers, in solution the UV-Vis spectra of P3a-c are characterized by broad absorption features, with the band at lower wavelength (below 400 nm) assigned to the π–π^* electronic transition of bithiophene donor units, and the band at higher wavelength (453–570 nm) related to the intramolecular π–π^* transition between the ground and the excited states of the donor- acceptor charge transfer complex (Figure 1).[36]
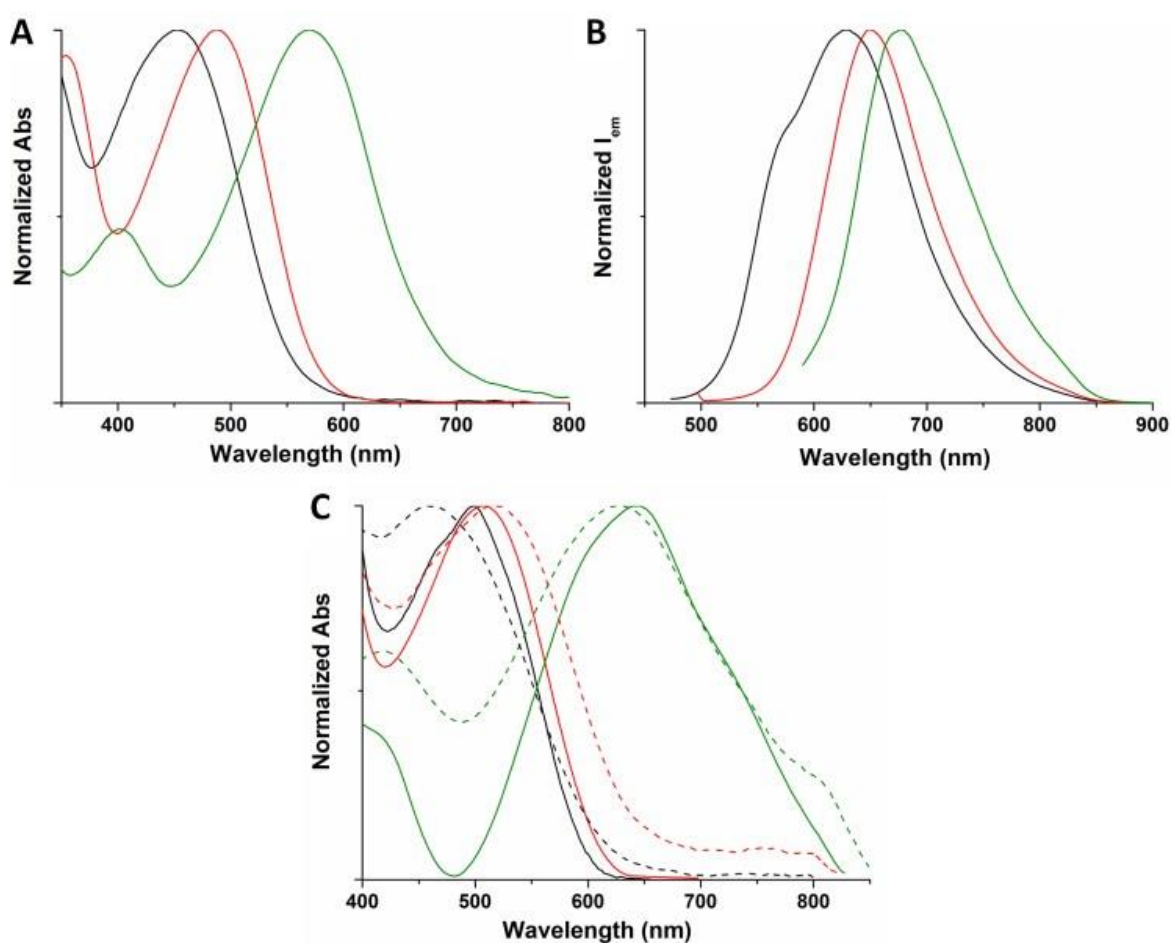

Figure 1. Normalized absorption (A) and photoluminescence (B) spectra in CHCl$_3$ of polymers (green line: P3a; red line: P3b; black line: P3c). Normalized absorption spectra (C) of polymers (green line: P3a; red line: P3b; black line: P3c) as films cast from chlorobenzene by the doctor-blade technique (solid line) and spray coating (dashed line).

As shown in figure 1A-B, P3a displays a remarkable bathochromic shift of the maximum of absorption and emission when compared to P3b and P3c because of the presence of oxygen directly linked to thiophene ring. Moreover, the lower Stokes shift of P3a is indicative of a reduced energy level of the excited state, related to the presence of a more ordered conformation of the macromolecules in solution promoted by the increased resonance in the main chain. The higher absorption and emission λ_{max} values of P3b with respect to P3c may be attributed to a higher polymerization degree of the former sample instead of an electronic effect by the side- chain methoxy-group on the aromatic system, since the absorption spectra of their precursors 3b and 3c are not shifted. (Figure S13). We also analyzed the UV-Vis spectra of thin films of the polymers deposited by doctor-blade and spray coating techniques from chlorobenzene. The UV- Vis spectra are reported in Figure 1C and the related data in Table 2. The absorption spectra of the polymers deposited by the doctor-blade technique appear significantly red-shifted if compared to the corresponding absorption spectra in solution and exhibit broader bands (Fig.1C). However, P3a displays a larger bathochromic effect (74 nm) with respect to the solutionthan P3b (20 nm) and P3c (47 nm). On the other hand, the spray coating technique produces thin films slightly red shifted with some further absorption bands at higher wavelength, in particular for P3a and P3b (Fig. 1C), probably because of more suitable conformations that better pack in the solid state. It is to be noted that, X-Ray reflectivity (XRR) and X-Ray diffraction (XRD) measurements, performed on all thin film polymer samples, indicate the absence of crystallinity (Figure S14). As reported in Table 2, the lowest optical energy gap values were found for the spray-coated thin films in agreement with electrochemical measurements, with P3a showing a value of 1.48 eV, which becomes close to 2 eV for P3b and P3c.

Table 2.Maximum absorption (λ_{max}) and emission (λ_{em}) wavelengths (nm) and optical energy gap of polymers P3a-c in CHCl$_3$ solution and in thin film deposited by doctor-blade or spray coating.

| | Solution | | | Thin film | | | |
| | | | | Doctor-blade | | Spray coating | |
Polymer	λ_{max} (nm)	λ_{em} (nm)	Stokes shift (nm)	λ_{max} (nm)	E_g^{op} (eV)	λ_{max} (nm)	E_g^{op} (eV)
P3a	570	677	107	644	1.53	629	1.48
P3b	487	650	163	507	2.03	516	1.93
P3c	453	629	176	500	2.10	454	2.03

Cyclic voltammetry measurements were carried out on thin film of P3a-c prepared both by doctor-blade and spray coating from chlorobenzene. The results are reported in Table 3 and the related voltammograms in Figure 2. It can be noted that the oxidation potential of the polymers is drastically reduced by the presence of oxygen in the side chain of thiophene rings regardless of the deposition method adopted. This effect is more pronounced for P3a (~0.4 V), in which the oxygen is conjugated with the thiophene ring, than P3b (~0.15 V) in which the oxygen is at the end of the side chain. The fact that P3b shows lower oxidation potential than P3c (~0.2 V)cannot be attributed to an electronic effect of the oxygen atom, as it is too far from the thiophene ring; however, the presence of oxygen as terminal may influence the intra- and interchain interactions of the side chains, increasing the polarity of the chains and decreasing the $\pi-\pi$ stacking distance of the backbone.[38,39] Differently, the reduction potential values appear rather insensitive to the chemical structure of the side chain substituent and strongly dependent on the deposition method. Indeed, the reduction potentials of polymers P3a and P3b deposited byspray coating method appear about 0.1 V more negative than those obtained by doctor blade,thus leading to lower energy gap values, particularly for P3a, in agreement with the results

obtained from the absorption spectra. As highlighted, the method employed for the preparation of the thin films causes a fine tuning of the energetic levels due to its impact on the resulting film morphology.

Table 3. Redox potentials, HOMO/LUMO energy levels and electrochemical energy gap values of the polymers.

Polymer	E_{ox}^{onset} (V vs. SCE)	E_{red}^{onset} (V vs. SCE)	HOMO (eV)	LUMO (eV)	E_g (eV)
P3a[a]	0.66	1.17	5.34	3.51	1.83
P3b[a]	0.87	1.16	5.55	3.52	2.03
P3c[a]	1.02	1.05	5.70	3.63	2.07
P3a[b]	0.62	1.05	5.30	3.63	1.67
P3b[b]	0.86	1.04	5.54	3.64	1.90
P3c[b]	1.03	1.07	5.71	3.61	2.10

[a] Polymers deposited by doctor-blade;[b] Polymers deposited by spray coating.
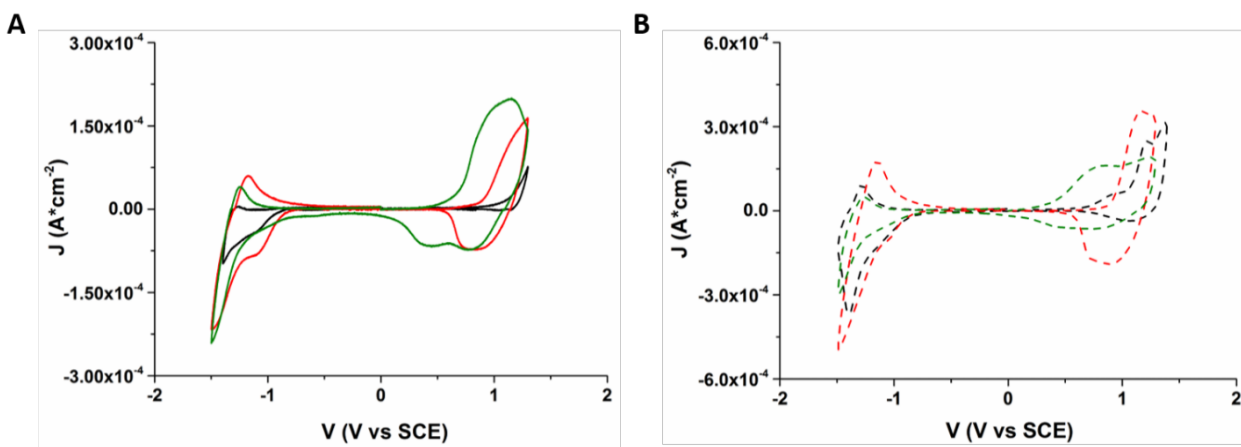

Figure 2. Cyclic voltammograms (second scans) in the solid state at 0.1 V s^{-1} of P3a-c films(green line: P3a; red line: P3b; black line: P3c) prepared by doctor blade (A) and spray coating (B) deposition.

3.3Photovoltaic properties. The photovoltaic properties of the polymers were tested in SMOSCs with structure ITO/PEDOT:PSS/photoactive polymer/Al. The J-V features of solar cells are reported in Figure 3 and the related photovoltaic parameters listed in Table 4. The film thickness of the three polymers range between $1.5\pm0.3\mu m$, as measured by profilometer.
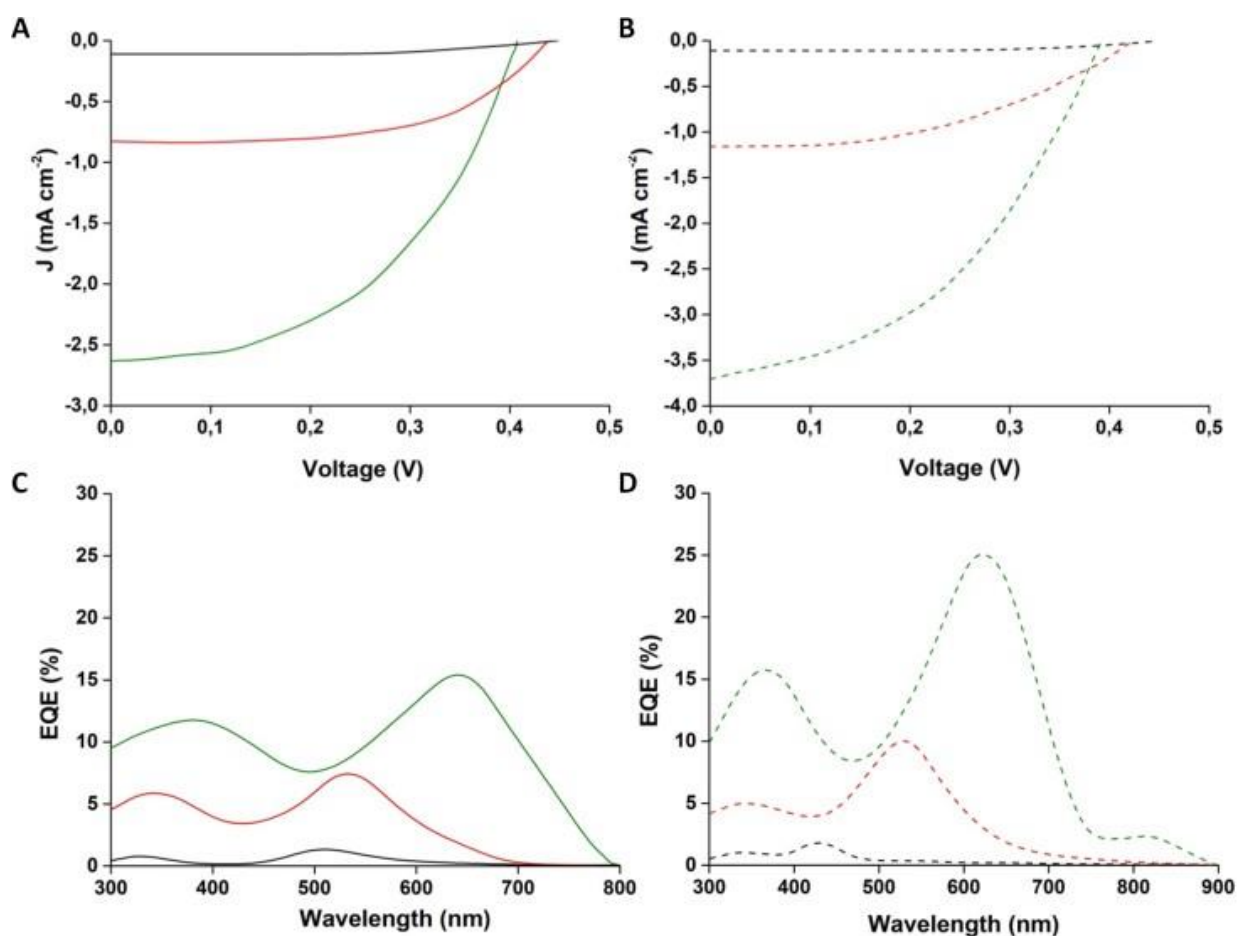

Figure 3. J-V characteristics under white light illumination of P3a-c cells prepared by doctor-blade (A) or spray coating (B) deposition (the best performing cells are displayed); EQE of the P3a-c cells prepared by doctor-blade (C) or spray coating (D) deposition. (green line: P3a; red line: P3b; black line: P3c).

As expected on the basis of energy gap values determined from optical spectra and cyclic voltammetry, the devices containing the photoactive component P3a and P3b deposited by spray

coating show the best efficiency results, achieving the maximum value of 0.77% with P3a and 0.21% for P3b; differently, P3c shows the lowest PCE value. Indeed, our results are primarily originated by the J_{sc} values, which are dependent on factors related to the efficiencies of each stage in the photovoltaic process, including the efficiency of light absorption, exciton diffusion, exciton dissociation, charge transport, and charge collection. They appear enhanced, mainly for P3a, with the spray coating procedure with respect the doctor-blade deposition. However, even ifthe V_{oc} values seem to be independent from the deposition method and the nature of thecompound, they are in good agreement with the trend observed for the electrochemical experiments carried out on the polymer thin films. Indeed, when the E_g value decreases, the V_{oc} -as being this parameter dependent to a first approximation on the difference between the HOMO of the donor and the LUMO of the acceptor - accordingly decreases. The overall cell performances of P3a and P3b result to be improved by the spray coating deposition, suggesting a more favorable arrangement of the macromolecules to exciton diffusion and charge transport. Moreover, it is also to be noted that the presence of oxygen in the side chain of P3b, although notdirectly involved in the aromatic conjugation, favours to some extent the photoconversion efficiency with respect to P3c. The external quantum efficiencies (EQE) of the cells (Figure 3) display maxima ranging from 15% (doctor-blade) to 25% (spray coating). The EQE values in theexamined range were used for calculation of J_{sc}, obtaining data (Table 7) consistent with the experimental findings, thus confirming the best performance of the device prepared with P3a by spray coating. Furthermore, the EQE profiles follow the trend observed in the UV-Vis spectra of polymers in thin film, indicating that the whole absorption effectively contributes to the photocurrent. It is also particularly noteworthy the wide range of absorption obtained for

P3adeposited by spray coating, that could be one of the factors on the basis of the high observed value of J_{sc}.

Table 4. Properties of organic solar cells prepared with polymeric derivatives P3a-c prepared by doctor-blade or spray coating technique (average values collected from ten devices).

Polymer	J_{sc} (mA/cm^2)[a]	J_{sc} (EQE)	V_{oc} (V)[b]	FF[c]	PCE (%)[d]
P3a[e]	2.63±0.09	2.59	0.41±0.01	0.51±0.016	0.55±0.035
P3b[e]	0.83±0.04	0.81	0.44±0.01	0.44±0.014	0.16±0.012
P3c[e]	0.11±0.01	0.11	0.45±0.01	0.41±0.014	0.02±0.011
P3a[f]	3.72±0.15	3.65	0.39±0.01	0.53±0.016	0.77±0.033
P3b[f]	1.16±0.09	1.07	0.42±0.01	0.43±0.012	0.21±0.016
P3c[f]	0.11±0.08	0.11	0.45±0.01	0.42±0.011	0.02±0.012

[a] Short circuit current; [b] Open circuit voltage; [c] Fill factor; [d] Photovoltaic cell efficiency; [e] By doctor-blade technique; [f] By spray coating deposition.

3.4Atomic force microscopy (AFM) and Kelvin probe force microscopy (KPFM) measurements. Since the electrical properties of the films strongly depend on their structure, we studied the surface morphology and the corresponding surface photo-voltage by AFM andKPFM techniques and the values are reported in Table 5. All three polymers deposited by spray coating exhibit a quite rough surface (R_{RMS}), ranging from ca 40 nm (P3a) to ca 100 nm (P3b, P3c), as depicted in the AFM images shown in Figure 4. Moreover, micrometric structures are present on the surfaces with different sizes, in particular, in the range of 0.2–2 μm for P3a, largerthan 5 μm for P3b and smaller than 1 μm for P3c. Maps of the surface density of photogenerated charges were measured by KPFM.[22,40-42] KPFM measurements are performed illuminating continuously all the samples (i.e. steady-state). We compared two different parameters: surface photovoltage (SPV) and SPV variance. The first parameter is defined as the difference between

the surface potential under illumination and in the dark: SPV = SPlight − SPdark and, solving the

Poisson's equation for electrostatics, SPV is correlated to the photocharge density.[26] Differently,

the SPV variance corresponds to the dispersivity of the measured data (i.e. the higher the SPV

variance, the lower the homogeneity of the photo-charge density). As observed, P3a film displays

higher values of both SPV and corresponding variance than the other two samples, P3b and P3c.

Thus, the presence of patches with different SPV reflects in larger SPV variance indicating that

the single material can be described as a heterojunction with regions with different charge

densities. This inhomogeneity in the photo-charges reflects in an overall higher SPV value clearly

showing a better intrinsic performances of the system respect to the other two materials.

Table 5. AFM and KPFM data for P3a-c.

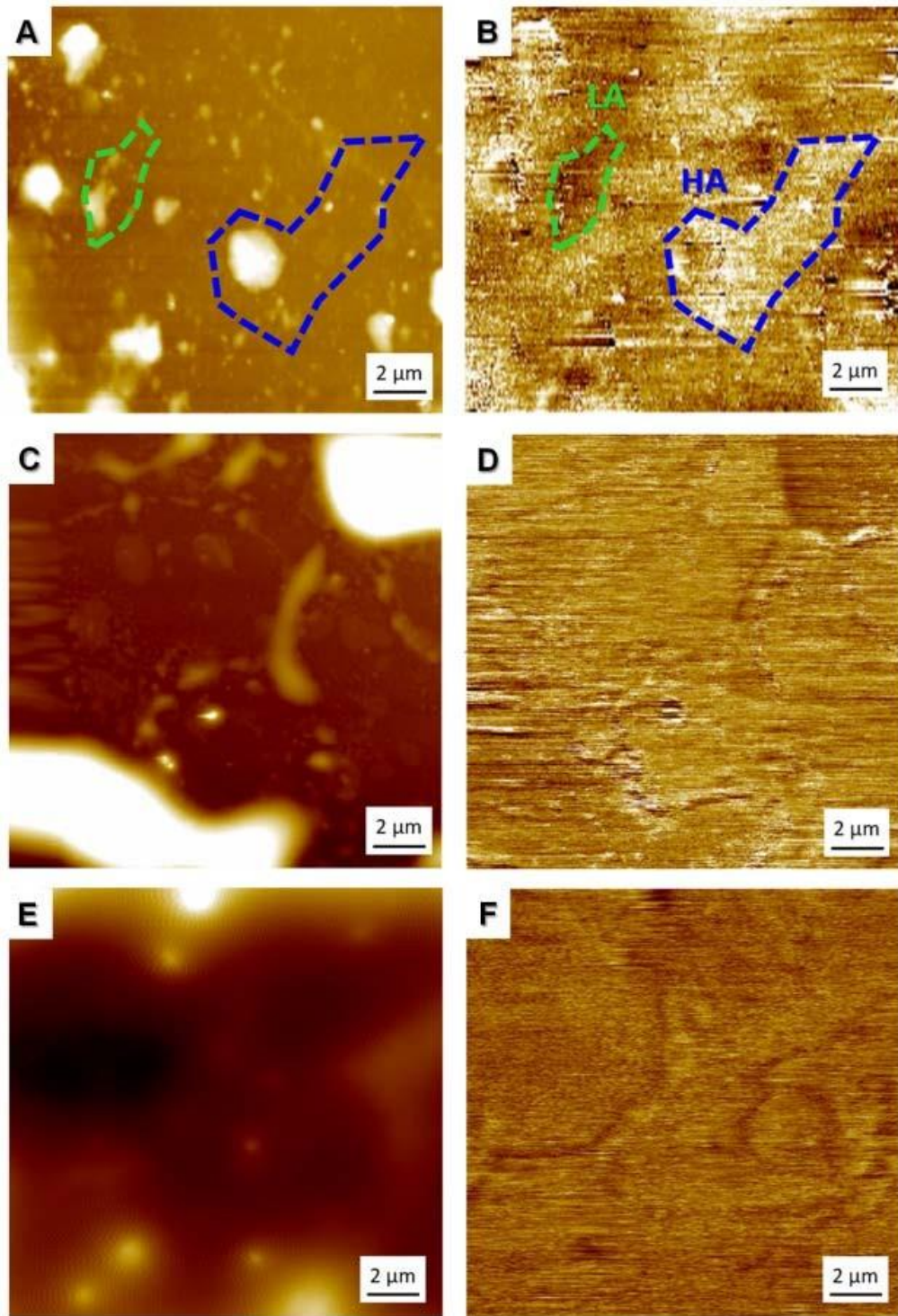| Polymer	R_{RMS} (nm)[a]	SPV variance (mV)	SPV (V)
P3a	40	480 ± 40	1.4 ± 0.2
P3b	100	170 ± 20	0.2 ± 0.1
P3c	100	100 ± 20	0.1 ± 0.1

[a] Standard deviation = 10%.

Figure 4. AFM (left, Z- range: 300 nm) and KPFM (right, Z- range: 1.2 V) images of P3a (A, B), P3b (C, D) and P3c (E, F).

4. CONCLUSIONS

Intrinsically regioregular linear D–A polymers - containing in the main chain alternating 4,4'-disubstituted bithiophene (D) and benzothiadiazole (A) moieties -have been prepared in good yields, through a straightforward oxidative polymerization process employing $FeCl_3$, and tested as active materials in SMOSCs. The side-chain substituent linked to the bithiophene moieties plays an important role, affecting significantly the optical properties, the energy levels and gap values of the material as well as their function as photoactive single components in solar cells. We show that the introduction of an oxygen atom in the alkyl side chain determines a wideningof the absorption band with a progressive red-shift, a reduction of the energy gap and a longer life-time of the generated photo-charges. In particular, we demonstrate that these effects are more pronounced when oxygen is directly linked to the thiophene unit (P3a). Its high electronegativity and mesomeric effect strongly influence the charge distribution over the molecule, light harvesting property and nanophase separation. Finally, we show that SMOSCs fabricated with the polymer P3a exhibit better performances in terms of photoconversion efficiency of sunlight than those fabricated with P3b, i.e., the polymer with the oxygen atom in a non-conjugated position with respect to thiophene unit, and P3c, i.e., the polymer withoutoxygen in the side chain, reaching significant values for fully conjugated alternating D–A system.[12] Moreover, in all cases the deposition of the polymers through spray coating method allowed to improve the PCE values, if compared to deposition by doctor blade. Indeed, the former method is likely to favour the formation of substructures on a nanometer scale that favours a more efficient separation of hole and electron transport.

CONFLICTS OF INTEREST

There are no conflicts to declare.

ASSOCIATED CONTENT

Synthesis of building blocks and polymers; ^{1}H and ^{13}C NMR spectra; TGA and DSC analysis; UV-PL spectra of monomers; X-Ray diffraction patterns.

REFERENCES

[1]   C. J. Brabec, N. S. Sariciftci and J. C. Hummelen, Adv. Funct. Mater., 2001, 11, 15-26.

[2]   L. Lu, T. Zheng, Q. Wu, A. M. Schneider, D. Zhao and L. Yu, Chem. Rev., 2015, 115, 12666-12731.

[3]   B. C. Thompson and J. M. Fréchet, Angew. Chem. Int. Ed., 2008, 47, 58-77.

[4]   Y. J. Cheng, S. H. Yang and C. S. Hsu, Chem. Rev., 2009, 109, 5868-5923.

[5]   J. Chen and Y. Cao,Acc. Chem. Res.,2009, 42, 1709-1718.

[6]   T. Xu and L. Yu, Mater. Today, 2014, 17, 11-15.

[7]   P. Zhou, Z. G. Zhang, Y. Li, X. Chen and J. Qin,Chem. Mater., 2014, 26, 3495-3501.

[8]   Y. Li, Acc. Chem. Res., 2012,45, 723-733.

[9]   R. Kroon, M. Lenes, J. C. Hummelen, P. W. Blom and B. De Boer, Polym. Rev., 2008, 48, 531-582.

[10] B. Xu, S. Noh and B. C. Thompson, Macromolecules, 2014, 47, 5029-5039.

[11] J. Roncali, Adv. Energy Mater., 2011, 1, 147-160.

[12] J. Roncali and I. Grosu, Adv Sci., 2019, 6, 1801026.

[13] Y. Huang, E. J. Kramer, A. J. Heeger and G. C. Bazan, Chem. Rev., 2014, 114, 7006-7043.

[14] P. Cheng and X. Zhan, Chem. Soc. Rev., 2016, 45, 2544-2582.

[15] N. Li, J. D. Perea, T. Kassar, M. Richter, T. Heumueller, G. J. Matt and N. S. Gu, Nat. Commun., 2016, 8, 14541.

[16] T. L. Nguyen, T. H. Lee, B. Gautam, S. Y. Park, K. Gundogdu, J. Y. Kim and H. Y. Woo, Adv. Funct. Mater., 2017, 27, 1702474.

[17]   A. Labrunie, J. Gorenflot, M. Babics, O. Aleveque, S. Dabos-Seignon, A. H. Balawi and P. M. Beaujuge, Chem. Mater., 2018, 30, 3474-3485.

[18] J. H. Lee, C. G. Park, A. Kim, H. J. Kim, Y. Kim, S. Park, M. J. Cho and D. H. Cho, ACS App. Mater. Interfaces, 2018, 10, 18974-18983.

[19] F. Pierini, M. Lanzi, P. Nakielski, S, Pawlowska, O. Urbanek, K. Zembrzycki and T. A. Kowalewski, Macromolecules, 2017, 50, 4972-4981.

[20] W. Lai, C. Li, J. Zhang, F. Yang, F. J. Colberts, B. Guo and M. Zhang, Chem. Mater., 2017, 29, 7073-7077.

[21] C. Guo, L. Yen-Hao, M. D. Witman, K. A. Smith, C. Wang, A. Hexemer, J. Strzalka, E. D. Gomez and R. Verduzco,Nano Lett., 2013, 13, 2957-2963.

[22] F. Di Maria, M. Biasiucci, F. P. Di Nicola, E. Fabiano, A. Zanelli, M. Gazzano, E. Salatelli, M. Lanzi, F. Della Sala, G. Gigli and G. Barbarella, J. Phys. Chem. C, 2015, 119, 27200-27211.

[23] S. Arumugam, D. C. Lacalle, S. Rossbauer, S. Hunter, A. L. Kanibolotsky, A. R. Inigo, P. A. Lane, T. D. Anthopoulos andP.J. Skabara, ACS Appl. Mater. Interfaces, 2015, 7, 27999-28005.

[24] A. Cravino, S. Roquet, O. Alévêque, P. Leriche, P. Frère and J. Roncali, Chem. Mater., 2006, 18, 2584-2590.

[25] F. Aziz and A. F. Ismail, Mater. Sci. Semicond. Process., 2015, 39, 416-425.

[26] F. Di Maria, M. Zangoli, M. Gazzano, E. Fabiano, D. Gentili, A. Zanelli, A. Fermi, G. Bergamini, D. Bonifazi, A. Perinot, M. Caironi, R. Mazzaro, V. Morandi, G. Gigli, A. Liscioand G. Barbarella, Adv. Funct. Mater., 2018, 28, 1801946.

[27] F. Di Maria, A. Zanelli, A. Liscio, A. Kovtun, E. Salatelli, R. Mazzaro, V. Morandi, G. Bergamini, A. Shafferand S. Rozen, ACS Nano, 2018, 11, 1991-1999.

[28] F. Di Maria, M. Zangoli, I. Palamá, E. Fabiano, A. Zanelli, M. Monari, A. Perinot, M. Caironi, V. Maiorano, A. Maggiore, M.Pugliese, E. Salatelli, G. Gigli, I. Violaand G. Barbarella,Adv. Funct. Mater., 2016, 26, 6970–6984.

[29] S. Trasatti, Pure Appl. Chem., 1986, 58, 955-966.

[30] G. Gratznerand J. Kuta, Pure Appl. Chem., 1984, 56, 461-466.

[31] J. Pommerehne, H. Vestweber, W. Guss, R. F. Mahrt, H. Bassler, M. Porsch and J. Daub, Adv. Mater., 1995, 7, 551

[32] C. M. Cardona, W. Li, A. E. Kaifer, D. Stockdaleand G. C. Bazan, Adv. Mater., 2011, 23, 2367-2371.

[33] A. Liscio, ChemPhysChem, 2013, 14, 1283-1292.

[34] C. Della Casa, P. Costa Bizzarri, M. Lanzi and F. Bertinelli, Acta Polym, 1997, 48, 251-255.

[35] R.H. Mitchell, Y.H. Lai and R.V. Williams, J. Org. Chem., 1979, 44, 4733-4735.

[36] A. A. El-Shehawy, N. I. Abdo, A. A. El-Barbary and J. Lee, Eur. J. Org. Chem., 2011, 25, 4841-4852.

[37] G. Barbarella, M. Zangoliand F. Di Maria inAdv. Heterocycl. Chem., Eds. E. Scriven, C. Ramsden, Academic Press, 2017, 123, 105-167.

[38] X. Chen, Z. Zhang, Z. Ding, J. Liuand L. Wang, Angew. Chem. Int. Ed., 2016, 55, 10376–10380.

[39] B. Meng, H. Song, X. Chen, Z. Xie, J. Liuand L. Wang, Macromolecules, 2015, 48, 4357–4363.

[40] A. Liscio, G. De Luca, F. Nolde, V. Palermo, K. Mullenand P. Samorì, J. Am. Chem. Soc., 2008, 130, 780-781.

[41] E. Salatelli, M. Marinelli, M. Lanzi, A. Zanelli, S. Dell'Elce, A. Liscio, M. Gazzano and F. Di Maria, J. Phys. Chem. C, 2018, 122, 4156-4164.

[42] A. Liscio, V. Palermoand P. Samorì, Acc. Chem. Res., 2010, 43, 541-550.